UNIVERSITY
OF WOLLONGONG
AUSTRALIA

University of Wollongong
Research Online

Faculty of Science, Medicine and Health - Papers

Faculty of Science, Medicine and Health

2012

Vanguard Cave sediments and soil micromorphology

Richard I. M Macphail
University College London

Paul Goldberg
Boston University, goldberg@uow.edu.au

R N. E Barton
University of Oxford

Publication Details

Macphail, R. I., Goldberg, P. & Barton, R. N. E. (2012). Vanguard Cave sediments and soil micromorphology. In R. N. E. Barton, C. B. Stringer & J. C. Finlayson (Eds.), Neanderthals in Context: a report of the 1995-1998 excavations at Gorham's and Vanguard Caves, Gibraltar (pp. 193-210). Oxford, United Kingdom: Oxford University School of Archaeology. © *Copyright 2012. Oxford University School of Archaeology and Individual authors - reproduced with permission.*

Research Online is the open access institutional repository for the University of Wollongong. For further information contact the UOW Library: research-pubs@uow.edu.au

Vanguard Cave sediments and soil micromorphology

Abstract
[extract] Introduction Vanguard Cave contains a sequence of over 17 m of deposits, generally made up of massive, coarse to medium sands interfingered with tabular to lenticular units of silts and silty sands (Fig 13.1).

Disciplines
Medicine and Health Sciences | Social and Behavioral Sciences

Publication Details
Macphail, R. I., Goldberg, P. & Barton, R. N. E. (2012). Vanguard Cave sediments and soil micromorphology. In R. N. E. Barton, C. B. Stringer & J. C. Finlayson (Eds.), Neanderthals in Context: a report of the 1995-1998 excavations at Gorham's and Vanguard Caves, Gibraltar (pp. 193-210). Oxford, United Kingdom: Oxford University School of Archaeology. © *Copyright 2012. Oxford University School of Archaeology and Individual authors - reproduced with permission.*

This book chapter is available at Research Online: http://ro.uow.edu.au/smhpapers/3083

13 Vanguard Cave sediments and soil micromorphology

R.I. Macphail, P. Goldberg and R.N.E Barton

Introduction

Vanguard Cave contains a sequence of over 17 m of deposits, generally made up of massive, coarse to medium sands interfingered with tabular to lenticular units of silts and silty sands (Fig. 13.1). The major body of sediment rests on a wave-cut platform preserved under a heavily cemented sand unit. The latter correlates with the raised beach deposits at the same elevation that form the base of the Gorham's Cave sequence. Most of the Vanguard sediments are calcareous with little diagenesis (Goldberg and Macphail 2000; Macphail and Goldberg 2000). In rarer cases, as in the Upper Area of the cave, the sands are interdigitated with black humic clays that display evidence of phosphatization. The paucity of visible karstic cave ornamentation (e.g. stalactites) suggests relatively dry conditions within the cave throughout most its history. The units of specific interest in this study are those that have produced human occupation evidence in the form of lithic artefacts, faunal remains and sometimes hearths or more diffusely defined combustion features. Four distinctive loci were investigated (Figs. 13.2 and 13.3).

Methodology

Several field and laboratory methods permit the detailed characterization of 'sediment types' according to a number of broadly defined attributes described below. Undisturbed samples for soil micromorphology were collected as small oriented blocks and in 30–40 cm long plastic downpipes (Fig. 13.4; Goldberg and Macphail 2006, fig. 15.13). Contexts, main stratigraphic units and layers within contexts were all sampled for bulk analyses in the field and also subsequently in the laboratory at the Institute of Archaeology, University College London.

Soil micromorphology

Undisturbed samples collected in the field were oven dried at 60°C and then impregnated with a crystic polyester resin diluted with styrene or acetone (Murphy 1986). After curing

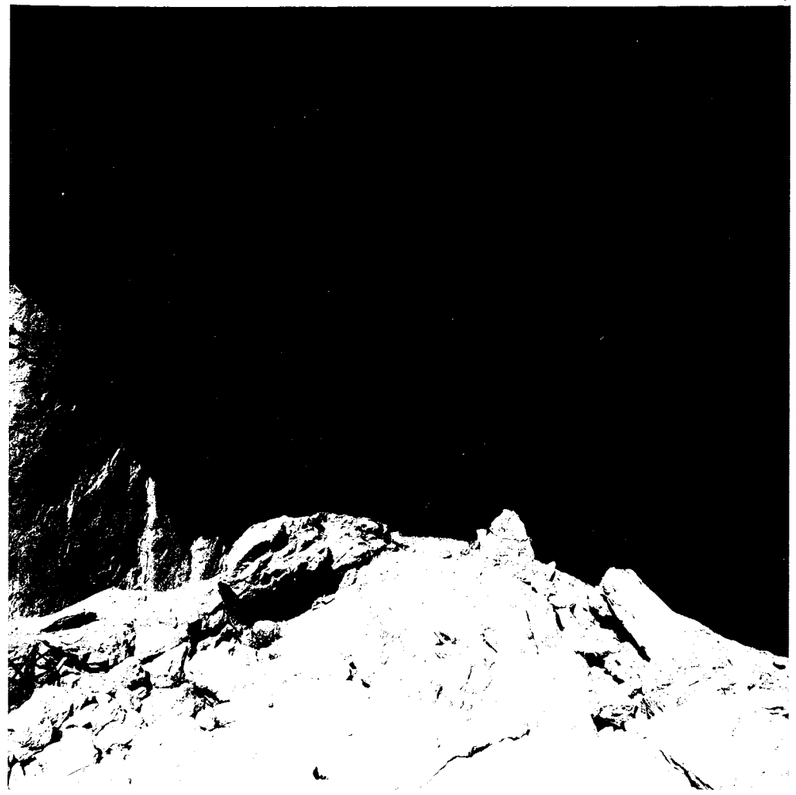

Fig. 13.1 Vanguard Cave. View of excavations in progress in the Middle Area of the main chamber (left) and of the Northern Alcove (right). Photo: Natural History Museum, London.

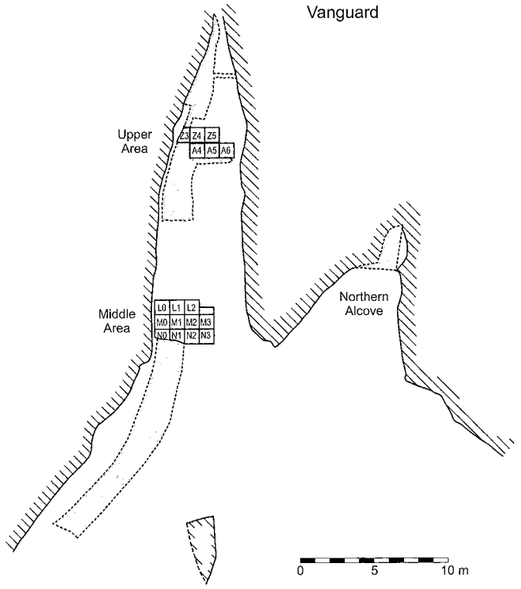

Fig. 13.2 Vanguard Cave. Plan location of excavated areas.

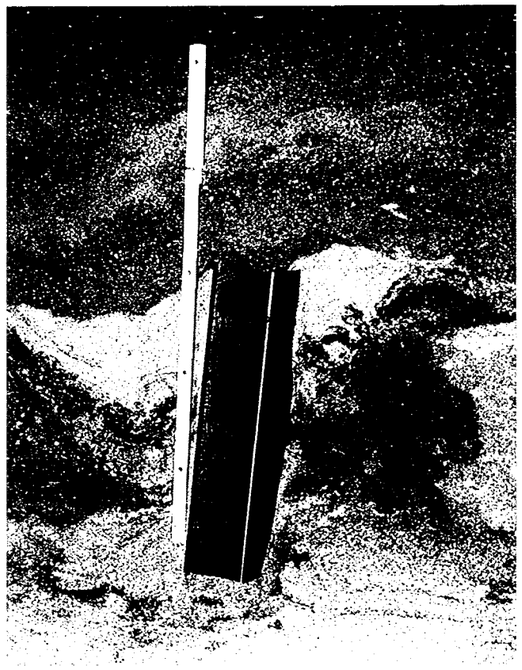

Fig. 13.4 Vanguard Cave Upper Area B. Position of long monolith sample 52, across sands and a possible guano/phosphate transformed combustion zone. Photo: R. Macphail and P. Goldberg.

for several weeks they were then placed overnight in an oven at 60°C. Slices from these blocks were manufactured into large-format thin sections (~4.5 × 7 cm observable area) by Spectrum Petrographics (Vancouver, WA, USA), or at the thin section laboratory of the Natural History Museum, London. Forty-two thin sections were made and described according to Bullock *et al.* (1985) and Courty *et al.* (1989). They were viewed at a number of magnifications from ×1, up to ×400 under a polarizing microscope, employing plane polarized light (PPL), crossed polarized light (XPL), oblique incident light (OIL), and blue light (BL) (cf. Stoops 1996; 2003, 24–25). The combined use of these different types of illumination permits a large number of optical inquiries to be made, for example forms of apatite (bone, guano and coprolites) which are autofluorescent under BL. The authors made extensive use of their own thin section reference collections and material from other cave studies (e.g. Meignen *et al.* 1989; Schiegl *et al.* 1996; Weiner *et al.* 1993; 1995).

Microchemistry

Micromorphological thin section data and bulk chemical findings were supplemented by microprobe analyses. Sediments from a column sample from the top of Area B (layers 52a, 52b and 52c) were subjected to microprobe (line and elemental map) studies (see below). This work was carried out at University College London, using a Jeol JXA8600 EPMA microprobe.

Table 13.1 Van 97/52, a 30 cm long column sample from near the top of Upper Area B (Fig. 13.4).

Context & sub-unit	Sediment description	Munsell colour
52a	Brown silt	7.5YR5/6 (strong brown)
52b	Tan sand	7.5YR7/4 (pink)
52c	Hard, cubic clay	10YR4/4 (dark yellowish brown)
52d	Brown crumbly clay/silt sand (includes burrow)	7.5YR4/4 (brown to dark brown)
52e	Light crumbly sand	7.5YR5/4 (brown)

Chemistry and magnetic susceptibility

Samples were analysed both at UCL, Institute of Archaeology (by Dr Cyril Bloomfield, retired from Rothamsted Experimental Station, Harpenden), and at Umeå University, Sweden (by Johan Linderholm). Bulk samples (<0.5 mm) were analysed for pH (2.5 H_2O), Loss-On-Ignition (LOI @ 550°C), total Phosphorus (P) employing ignition, HCl pre-treatment and 2N nitric acid extraction (UCL) and low frequency magnetic susceptibility (χ) studies at Umeå University, Sweden (Holiday 2004, appendix 2; Linderholm 2007).

Upper Area

The sands of the upper sequence extend almost to the cave roof, some 30 m from the present dripline (Fig. 13.3). As in other parts of the cave the sediments can be divided into buff- and pink-coloured (7.5YR7/4 – moist) sands interstratified with lenses of dark brown (7.5YR4/4 – moist) silts and silty sands (Figs. 13.5 and 13.6). The latter include a wash component, with transient pooling, followed by desiccation cracking. Similar phenomena have also been noted in various levels of Gorham's Cave (cf. LBSm). In some places the darker lenses are capped by consolidated crusts that can be traced back into the cave as continuous surfaces. The uppermost dark lenses investigated (contexts 50–55; Figs. 13.7–13.9) yielded some rare faunal remains including wild pig but no *in situ* artefacts. In Upper Area B, a 30 cm long column sample Van 97-52 was examined in detail (Table 13.1; Fig. 13.4).

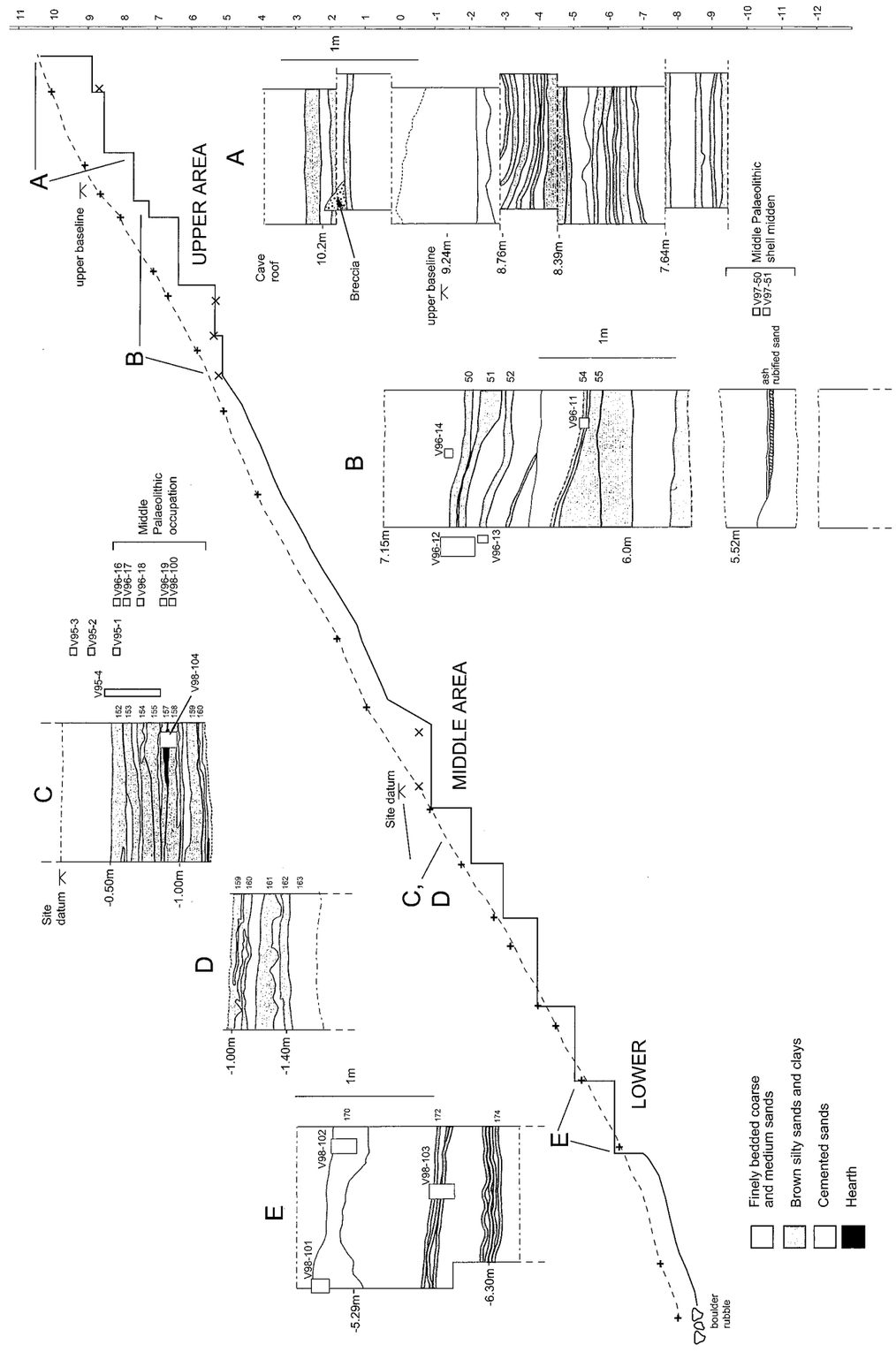

Fig. 13.3 Vanguard Cave. Axial cross-section through the cave showing main excavated areas (A–E) and stratigraphic units, indicating micromorphology sampling points.

Fig. 13.5 Vanguard Cave Upper Areas A and B facing back of cave. Foreground: Area B from base of context 54. Photo: Natural History Museum, London.

Five sub-divisions of layer 52 were identified and examined through soil micromorphological thin section and bulk studies. Microprobe analysis of sample layers 52b and 52c was carried out because this location appeared to be the best expressed area of guano concentrations at Vanguard Cave. In contrast to Gorham's Cave, guano and phosphate features are relatively uncommon.

The first horizon with recognizably Middle Palaeolithic finds is situated about 5.4 m above datum in Area B (Fig. 13.10). It is marked by a pinkish-grey ashy deposit resting on more consolidated silty sands that can be followed for a few metres as a sub-horizontal surface dipping gently towards the back of the cave. The presence of a hearth is indicated by pinkish grey (7.5YR7/2) ash (~1.5 cm thick), overlying buff- coloured silty sands that are characterized in places by a 10 mm thick reddening or rubefaction (reddish brown 5YR5/4) where the sediments have been altered by heating. The hearth (sample Van 97-51) (Fig. 13.11) is associated with a scatter of burnt marine shells and a concentration of knapping debris, and is interpreted as the remains of activities involving the processing of marine foods by Neanderthals (Barton 2000; Fernández-Jalvo and Andrews 2000; Stringer *et al.* 2008). Also present in the ashy deposits were a number of animal coprolites that are reported in Chapter 19. The Middle Palaeolithic artefacts associated with this surface are described in Chapter 20.

Middle Area

The Middle Area is located close to where we placed the site datum, about half way up the cave sequence and 15 m in from the present dripline. The deposits in this part of the cave are also characterized by alternating bands of finely bedded coarse and medium sands interdigitated with brown silts and clays (Table 13.2; Fig. 13.12). The bands are associated with a number of well defined, discrete archaeological horizons. There is a major sand unit between the Middle and Upper Areas consisting of coarse and fine sands that we tested but were found to be more or less archaeologically sterile.

The deposits in this area on the south side of the cave were examined in detail. They revealed at least 12 separate pairs of brown silty sand and lighter sand bands which formed

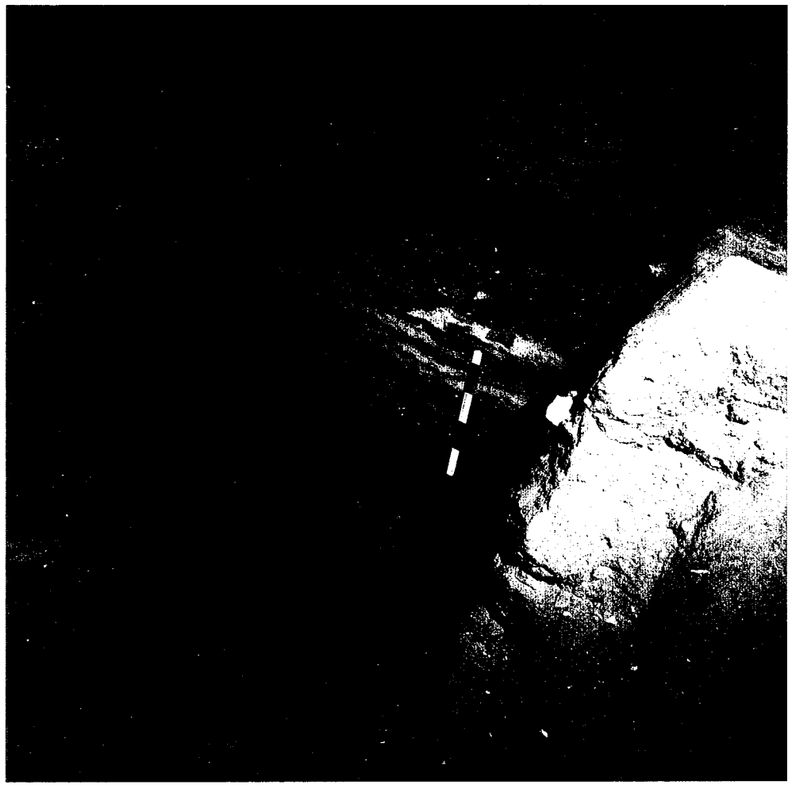

Fig. 13.6 Vanguard Cave Upper Area A. Darker and lighter bands of silts and silty sands. Photo: Natural History Museum, London.

Fig. 13.7 Vanguard Cave Upper Areas A and B. The string in the foreground marks the top of context 54. The two overlying darker bands indicate contexts 52 and 50 (top). The long monolith sample was taken across context 52. Scale bar in 10 cm. Photo: Natural History Museum, London.

Fig. 13.8 Vanguard Cave Upper Area B. Similar view to 13.7. It shows 'desiccation surfaces' of context 54, with 25 cm scale bar, and contexts 52 and 50 above. Photo: Natural History Museum, London.

Fig. 13.9 Vanguard Cave Upper Area B. View from above showing 'desiccation surfaces' of context 50 (upper) and context 54 (lower). Photo: Natural History Museum, London.

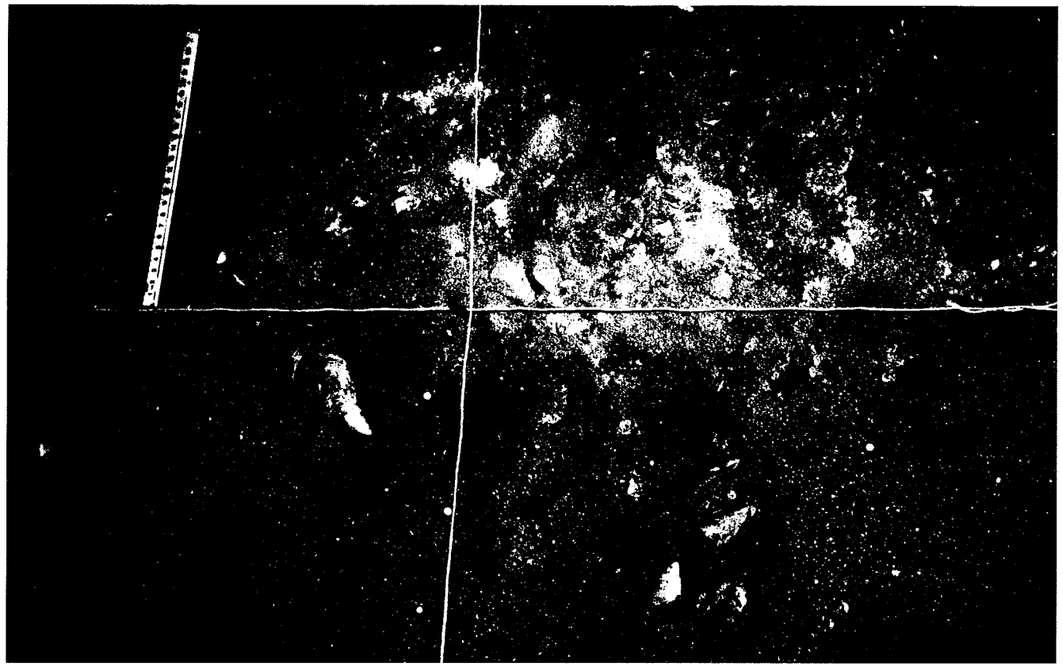

Fig. 13.10 Vanguard Cave Upper Area B. Image of Middle Palaeolithic shell midden. Photo: Natural History Museum, London.

more or less continuous compact surfaces that could be followed as they dipped gently towards the back of the cave. Finds of lithic artefacts and bone seemed to be concentrated mainly within these silty sub-units, the intervening sands being more or less devoid of any archaeological material. Each of the silt and sand pairs was described as a 'context' (Table 13.2). We interpreted those with artefacts as forming occupation episodes separated by small accumulations of clean blown sand, the latter probably representing relatively short interruptions in the silty sequence. According to the refitting of bones between different contexts (Chapter 21), the deposits appear to have been disturbed very locally by such processes as small-scale burrowing.

Individual charcoal-rich hearths and more diffuse combustion horizons were recorded within the brown silty sands and clay layers. The most completely excavated sample occurred within contexts 157–158 (Fig. 13.13). This large hearth was given the context number 150 (Table 13.2; Fig. 13.14). A sediment column was obtained through this feature which revealed two dark reddish brown organic-rich layers (each ~2 cm thick) separated by a possible ash layer about 1 cm thick (Table 13.3); the five units (150a–150e) were analysed for total Phosphorus and LOI (see Table 13.6, samples 19a–19e). Much charcoal was noted in the silty clay sediments and appeared widespread over an area some ~60 cm in diameter.

In contrast to the large hearth (150) a more enigmatic combustion feature was also investigated (context 156). It was interpreted as the remnants of a hearth or a localized inwash fill from a nearby hearth. Five sub-units were identified in the monolith box and the sediments were tested for magnetic susceptibility (see below and Table 13.4).

Fig. 13.11 Micromophology sample Van 97/5l thin-section scan. Upper Area B shell midden and hearth. Note 15 mm of ash over reddened sands containing shell fragments that recorded diminishing magnetic susceptibility through undisturbed hearth deposits. Width is ~50 mm. Photo: R. Macphail and P. Goldberg. (Colour versions of all thin sections available online)

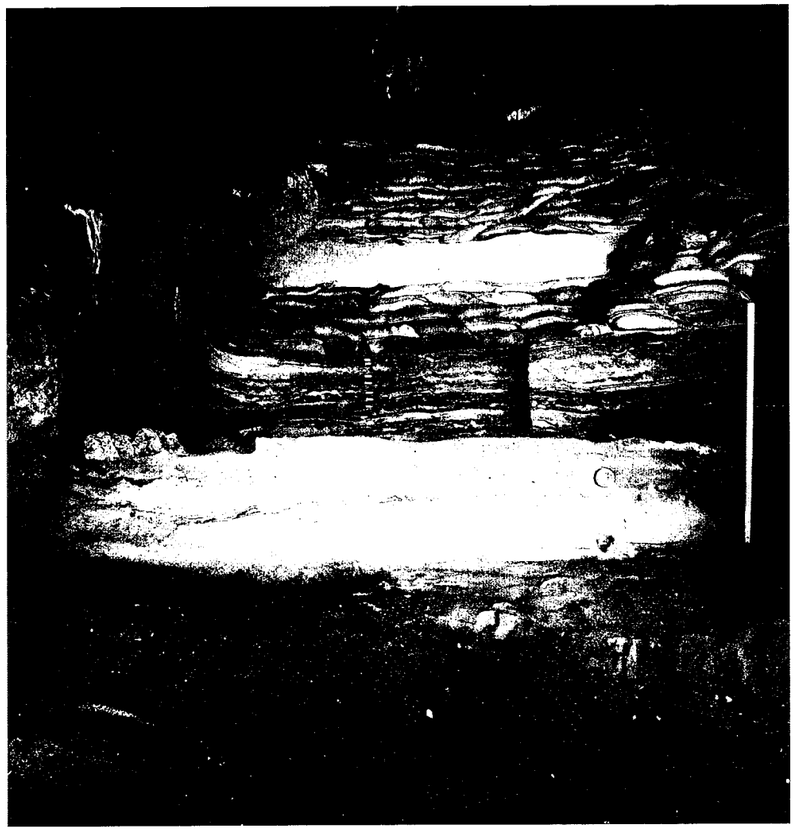

Fig. 13.12 Vanguard Cave Middle Area. Interdigitated sands and silts. The hearth feature (context 150) is just visible in the labelled section as a darker patch of silt. Two OSL samples (OSL 98/4 and OSL 98/5) can be seen in the foreground. The site datum can be seen as the nail at the centre of a white-painted T on the south wall of the cave. Photo: Natural History Museum, London.

Table 13.2 Vanguard Middle Area. Stratigraphic sub-divisions and 'contexts' and showing the concordance between unit labels from different seasons.

Contexts	Sediment	Sediment descriptions	Unit nos. used in 1995–6	Context nos. used in 1997–8	Context descriptions
152	Sand	Yellow-brown sand	100		
	Sand	Pink sand	101		
	Silt	Dark brown clayey silt + sands	102	52	
153	Sand	Pale pink/yellow coarse sands	103	53	
	Silt	Dark brown clayey silt	104	53	
154	Sand	Pinkish coarse-medium sands	105	54	
	Silt	Dark brown clay sand	106	54	
155	Sand	Pink coarse-medium sand	107		
	Silt			55	Brown clayey silt containing C[1] (156)
157	Sand	Dark brown clayey sand			
	Silt		108	57	Dark brown clayey sand + sand lenses containing Large hearth H[2] (150)
151	Silt		108 lower		Dark brown clayey sand underlying H
158	Sand	Pink coarse-medium sand	109	58	Pink coarse-medium sand
	Silt				Brown clayey silt
159	Sand			59	Pink coarse-medium sand
	Silt				Brown clayey silt
160	Sand			60	Pink coarse-medium sand
	Silt				Brown clayey silt
161	Sand			61	Pink coarse-medium sand
	Silt				Brown clayey silt
162	Sand			62	Pink coarse-medium sand
	Silt				Brown clayey silt
163	Sand			63	Pink coarse-medium sand
	Silt				Brown clayey silt

1 Shallow depression with charred base (C-Combustion feature = context 156).
2 Large hearth (H) (= context 150).

Table 13.3 Van 96/19, a monolith box sample through the large hearth (context 150).

Context & sub-unit	Sediment description	Munsell colour
150a	Charcoal-rich dark reddish brown clay	5YR3/2
150b	Brown ashy	7.5YR5/4
150c	Dark reddish brown, part burned clay	5YR3/2
150d	Reddish brown, rubefied clay	5YR4/4
150e	Strong brown silty clay	7.5YR5/6

Table 13.4 Van 97/54, a monolith box sample through combustion feature (context 156).

Context & sub-unit	Sediment description	Munsell colour
156a	Reddish brown silts	5YR4/4
156b	Dark reddish brown silts	5YR3/2
156c	Strong reddish brown silty clay	7.5YR4/6
156d & e	Yellowish brown sand	5YR4/6

Lower Area

A trench contiguous with the Middle Area deposits was extended down to approximately 6.5 m below datum beyond the cave entrance drip line and near the rock-cut platform close to present sea-level. Only in Area E were a series of well defined light brown clay bands with intervening clean sands recorded (Fig. 13.3). Apart from some isolated faunal remains (none with cut-marks) there were no artefacts.

Northern Alcove

Excavation was undertaken on the north side of the main chamber (Figs. 13.2 and 13.15). The sediments in this area are characterized by more massive sands punctuated by numerous reddish brown clay and silt stringers that thin in a direction away from cracks in the cave walls. It suggests that the brown silty units, e.g. sample Van 97-53 (Figs. 13.16 and 13.17), here and more generally within the cave, were washed in along joints and fissures of the bedrock. In the alcove area the sands were much less consolidated and the banding more diffuse than elsewhere in the main sequence. The sediments lay at more or less the same altitude as the deposits of the Middle Area and may have formed continuous layers, although no attempt was made to link the two areas stratigraphically. Only relatively few archaeological finds were recovered in the Northern Alcove. One of the more important features recorded in this area, however, was a small oval hearth measuring about 50 × 25 cm (Fig. 13.18; Table 13.5). It consisted of a 1–2 cm thick layer of laminated ash overlying a further 2 cm thickness of burnt sand and charcoal with some patches of underlying rubified sand. With the exception of a few scattered flakes there was no other evidence of human activity in the sediments immediately surrounding the hearth. A few artefacts were recorded from lower down in the sequence but not in any great density (Fig. 13.19).

Sediment micromorphology, chemistry and magnetic susceptibility

The aim of this study was to assess site formation processes using a combination of thin section, microchemistry, bulk chemical and magnetic susceptibility analyses in cave sediments composed dominantly of sand, silt and some guano. It permitted the detailed characterization of sediment types according to a number of broadly defined attributes, such as micro-facies (including components, grain size and sorting, microfabric type), and chemical and magnetic signature.

Table 13.5 The Northern Alcove. Stratigraphic sub-divisions and 'contexts'.

Contexts 1996–7	Unit Number 1995–6	Sediment description
1000	500	Brown clayey silt. Bioturbated, homogeneous with infrequent sand lenses
1001	500	Coarse sand, yellowish brown with broken shells (bioturbated)
1002	501	Two consolidated narrow dark brown bands of sandy clayey silt
1003	502	Coarse sand light yellow/brown
1004	503	Narrow dark brown clayey silt
1005	504	Light brown, coarse sandy layer. HEARTH at interface of 504/505
1006	505/506	Dark brown clayey silt
1007		Light yellowish brown sand
1008		Light yellowish brown sand with brown clayey silt, probably mixed
1009		Dark brown clayey silt
1010		Undescribed
1011		Light yellowish brown sand
1012		Dark brown clayey silt
1013		Light yellowish brown sand (heavily bioturbated)
1014		Dark brown clayey silt with thin intervening light yellowish sand band
1015		Light yellowish brown sand
1016		Dark brown clayey silt
1017 1018		Light yellowish brown sand with thin continuous lenses of dark brown clayey silt
1019		Light yellowish brown sand
1020		Dark brown clayey silt (discontinuous)
1021		Light yellowish brown sand and overlying band of dark brown clayey silt
1022		Light yellowish brown sand and overlying band of dark brown clayey silt
1023		Dark brown clayey silt

Soil micromorphology results

Sediment types are grouped according to their facies and sub-facies characteristics, namely,

- ***S* Sands**: clean fine- to medium-size sands; massive to very coarsely bedded, commonly well sorted, with few charcoal, and very few humic and excremental inclusions (Fig. 13.20). A variant of this is moderately sorted sands containing land snail shell fragments.
- ***Si* Silts**: calcitic and non-calcitic silts; finely bedded, commonly well sorted with few fine sand, charcoal and few humic fragments (Figs. 13.20 and 13.14). Variants include a calcitic, in places probably ashy, fine fabric, and planar pseudomorphs of plant fragments (sample Van 97-53; Figs. 13.16 and 13.17).
- ***G* Guano**: the guano facies is composed dominantly of two sub-facies. Subtype *Gi* is heterogeneous, reddish brown, porous, highly humic and excremental (burrowed) in character, and may contain inclusions of bone,

Fig. 13.13 Vanguard Cave Middle Area. Image of Middle Palaeolithic hearth (context 150) set in dark silts (samples Van 96/19 and Van 98/104); a vertical sequence of bulk analyses (sample layers a–e) were also taken through the hearth. Photo: P. Goldberg and R. Macphail.

charcoal and plant fragments. Irregular-shaped, amorphous material, sometimes containing plant material and autofluorescent under BL, may also occur as inclusions (sample Van 52c; Table 13.6). The second type, *Gii*, is homogeneous, pale grey, massive/bedded, non-birefringent, and is highly autofluorescent under BL (sample Van 52c; Table 13.6; Figs. 13.21–13.28). It is similar to secondary phosphates observed in other prehistoric caves in the Mediterranean region (Weiner *et al.* 1995; Schiegl *et al.* 1996).

***H* Hearths and Combustion features**: variants include rubified, finely bedded silts (Si) and can contain sand, fine charcoal, charred organic matter, burned bone and ash crystals (e.g. sample Van 97-54 Middle Area (context 156); Figs. 13.29 and 13.30). In the case of sample Van 97-51 (Upper Area 'B'), weakly rubified sands (S) occur, with a 10–20 mm thick ash layer composed of micritic remains of wood ash (but no phytoliths) (see Figs. 13.11, 13.31 and 13.32). This ash exhibits

Fig. 13.14 Micromophology sample Van98/104 thin-section scan. Middle Area context 150, showing rubefied hearth deposits (facies *CZ*) sealed by ensuing silt-dominated sediments (facies *Si*) themselves intercalated with sand (sub-facies *S*). Width is ~50 mm. Photo: R. Macphail and P. Goldberg.

pseudomorphs of very thin burrows and broad excrements (including biogenic calcite). Bedding and welding of micrite and the increasing abundance upwards of sand testify to exposure and weathering of the hearth followed by relatively rapid burial by blown sand.

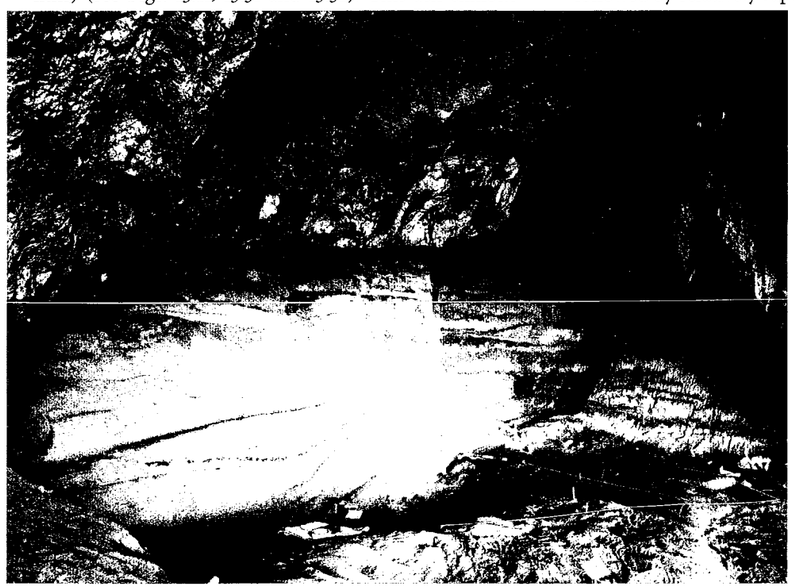

Fig. 13.15 Vanguard Cave Northern Alcove, viewed west and showing small hearth feature (context 1005) indicated by scale bar. Photo: Natural History Museum, London.

Table 13.6 Bulk data associated with sediment and micro-facies types identified in thin section at Vanguard Cave.

Samples	Sediment Types	Facies types	Total P ppm	MS (χ x 10-8 Si/Kg)	pH (H_2O)	% LOI
Van 97/51a	H	A/S		76		
Van 97/51b	H	A/B/S		31		0.3
Van 97/52a	S	S	1880			2.5
Van 97/52b	S	S	850			1.1
Van 97/52c	G	G/OM/S	18000			3.9
Van 97/52d	S	S	760			1.3
Van 97/52e	S	S	2300			1.2
Van 97/54a	H	S/OM (G, C, A)		234		2.4
Van 97/54b	H	S/A/OM (B, C)		223		3.8
Van 97/54c	H	S/A		128		2.5
Van 97/54d	S	S		90		1.8
Van 96/13	Si	S/Si/OM		98	8.1	2
Van 96/16	Si	Si (OM)		99	8.1	2.6
Van 96/17	Si	Si/S (OM)		63	7.8	1.3
Van 96/18	Si	S/Si (OM)		93	8.3	1.8
19a	H	S/OM (G, C, A)	3210			3.3
19b	H	S/A/OM (B, C)	4860			2
19c	H	S/OM (G, C, A)	2300			3
19d	H	S/OM (A, B)	2060			1.6
19e	H	S/OM (G, C, A)	3060			2
53	Si	Si	1740	107		0.55
Van 98/100		C		72	7.8	2.6
Van 98/101	S	S/Si		22	8.6	0.7
Van 98/102	S	S/Si		14	8.7	0.8
Van 98/103	Si	S/Si (A?)		22	7.8	1.3

Key to Sediment (Facies) type:
H – Hearth/Combustion Zone, G – Guano, S – Sands, Si – Silts.
Key to micro-facies present:
A – ash, B – burrows (biological activity), C – charcoal,
Ca – secondary calcium carbonate, G – guano, OM – organic matter,
S – sands, Si – silts.

In Table 13.6 further information is presented on the different micro-facies of the sediment types.

Chemical and magnetic susceptibility results

These are presented in Table 13.6 and with data from V97-54 (context 156, combustion feature; see Table 13.4 and

Fig. 13.16 Micromorphology sample Van97/53 (Northern Alcove). Photomicrograph of interbedded silts (micro-facies *Si*) and sands (micro-facies *S*) that records inwash of fine (silt and clay) soil through the cave's karstic system (possibly seasonally) and sand blowing from coastal dunes. PPL, width is ~3 mm. Photo: R. Macphail and P. Goldberg.

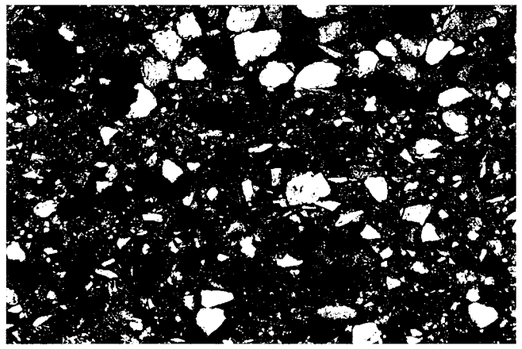

Fig. 13.17 As Fig. 13.16, employing XPL; note that even the silts can include wind-blown sand grains. Photo: R. Macphail and P. Goldberg.

Fig. 13.33a and b). All sediments are alkaline (mean pH 8.1, range pH 7.8–8.6). Scattergrams were employed to compare the sediments of Vanguard and Gorham's Caves (Macphail and Goldberg 2000). Generally, the sediments from Gorham's Cave have higher amounts of phosphate and organic matter, but a similar range of magnetic susceptibility values,

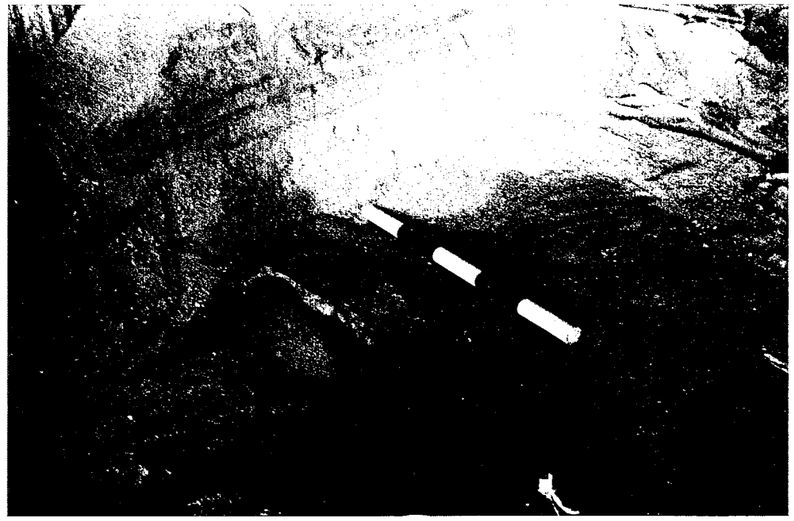

Fig. 13.18 Vanguard Cave Northern Alcove. Close up of small hearth feature (context 1005). Cross section left of the nail in the foreground. Photo: Natural History Museum, London.

Fig. 13.19 Vanguard Cave Northern Alcove. View of sediments below context 1006. One metre scale. Photo: Natural History Museum, London.

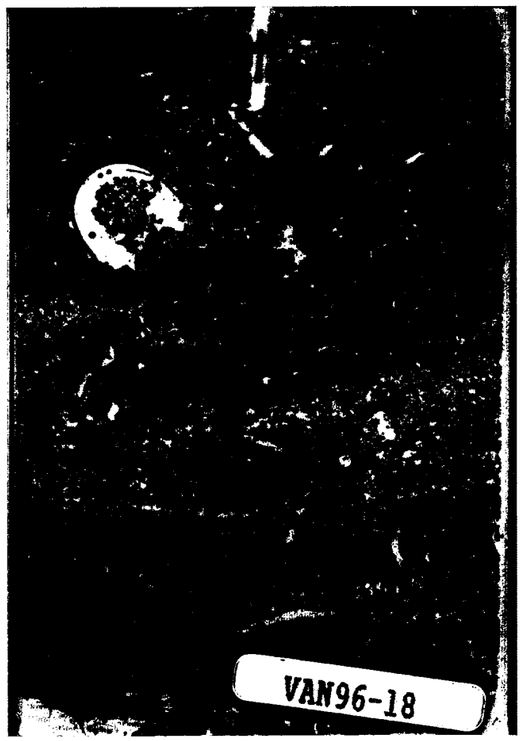

Fig. 13.20 Micromorphology sample Van 96/18 thin-section scan. This shows dominant silts (facies *Si*) with interbedded sands (sub-facies *S*) in Middle Area of cave at approximately context 154 (see Table 13.2). Frame width is ~50 mm. Photo: R. Macphail and P. Goldberg.

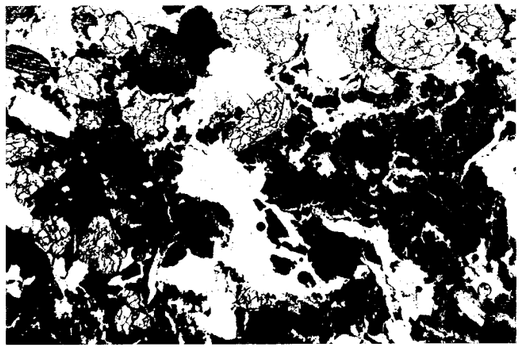

Fig. 13.21 Photomicrograph of mixed guano (micro-facies *Gi*) from Van 97/52 (Upper Area), showing dark reddish phosphate crust below a blown sand layer. It is possible that the dark reddish colours are indicative of heating consistent with the presence of charcoal in this context (see Fig. 13.32). PPL, frame width is ~3 mm.

as compared to those of Vanguard Cave. Low amounts of organic matter occur at Vanguard Cave (mean 2% LOI; max. 3.9% LOI), with the highest amounts associated with 'Guano' (3.9% LOI) and 'Combustion Zones' (3.8% LOI), compared to 'Sand' (0.7–2.5% LOI) and 'Silt' (0.5–2.6% LOI) sediment types. Equally, these ('Sand': 760–1880 ppm P; 'Silt': 1740 ppm P) are less rich in P compared to 'Combustion Zones' (2060–4860 ppm P), and very much less enriched in P compared to a 'Guano' layer (18,000 ppm P) (see microchemistry). Some high magnetic susceptibility values are coincident with known 'Combustion Zones' (CZ: max. 234 $\chi \times 10^{-8}$ Si/Kg) compared to 'Sand' (14-90 $\chi \times 10^{-8}$ Si/Kg) and 'Silt' (22-107 $\chi \times 10^{-8}$ Si/Kg) sediment types, but it

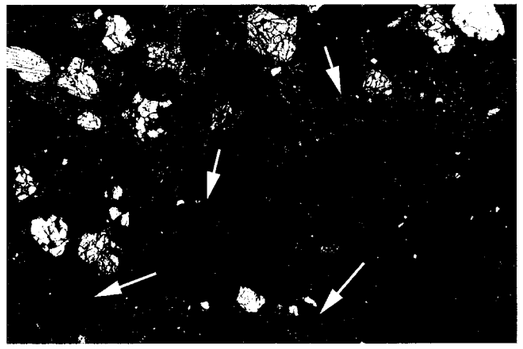

Fig. 13.22 As Fig. 13.21, in XPL, showing isotic organic matter-stained phosphate (P-Ca-Fe-Mn), with possible calcitic traces (arrows) as evidence of an earlier existing combustion zone (possibly ashes) here; deposition of guano led to the phosphatization of this hearth. Photo: R. Macphail and P. Goldberg.

can be noted that ash-rich layers show poor enhancement (sample 51b) presumably because of the lack of ferruginous mineral matter.

Microchemistry results

Quantitative microprobe analysis was performed on the column sample from the top of Area B (layers 52a, 52b and 52c; see Tables 13.1 and 13.6). These samples come from a microfabric within a 'Guano' (G) type sediment and were analysed by elemental mapping and by line analysis. They yielded mean values of 9% Si, 7% Ca, 2.9% P, 1.8% Al, 1.5% Fe and 0.8% Mn (n=227), with maximum values of 41% Si, 36% Ca, 14% P, 35% Al, 27% Fe and 42% Mn, respectively. Layer 52a (type Gi) although dominated by Ca-P contains biologically mixed layers and fragments of Fe-rich material (Figs. 13.23 and 13.24). In contrast, layer 52b (type Gii) is composed of layers of little disturbed Ca-P (presumed to be pure guano formed of hydroxyapatite) with intercalated Fe-Mn (relict of organic matter?) and layers of mixed Al-Si-Fe-Mn cave earth (Figs. 13.25–13.27). Layer 52c (type Gi) is heterogeneous and contains patches again rich in Ca-P biologically mixed with areas of Fe-Mn (Fig. 13.28).

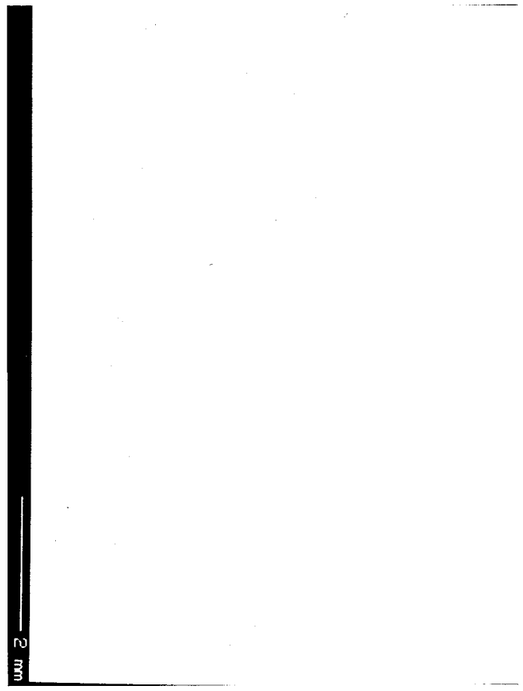

Fig. 13.23 Microprobe elemental map: Van 97/52, layer 6b; P in guano – micro-facies *Gi*. Frame width is ~9 mm. Photo: R. Macphail and P. Goldberg.

Fig. 13.24 As Fig. 13.23, microprobe elemental map: Van 97/52, layer 6b; Fe-P-Ca in guano – micro-facies Gi. Phosphorus mapped as P (1.07%), P-Ca (26.88%), P-Fe (0.49%) and P-Fe-Ca (9.41%), with 1.61% Ca and mixed layers of (23.19%) Fe. Frame width is ~9 mm. Photo: R. Macphail and P. Goldberg.

Discussion

The identification and recognition of sediment facies and micro-facies types permit us to extend our interpretations of site formation processes and human activities at Vanguard Cave. These are discussed in terms of the major sediment (facies) types.

S* *Sands: Clean, well-sorted, fine to medium sands are likely to reflect episodes of dry conditions and wind-blown deposition of sands from coastal dunes present along the coastline when sea-levels were lower than today (Davies *et al.* 2000; Finlayson and Pacheco 2000). This origin and mode of deposition is reflected in their low LOI (Loss-On-Ignition) phosphate content and magnetic susceptibility values. The sands can contain rounded sand-size shell, limestone and fossil fragments

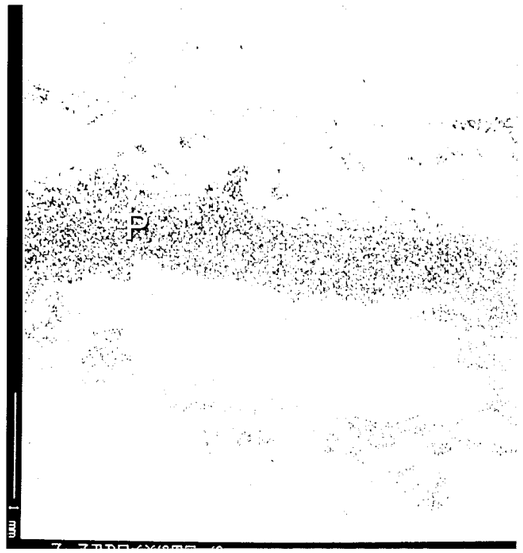

Fig. 13.25 Microprobe elemental map: Van 97/52, layer 6a; P in guano – micro-facies *Gii*. Frame width is ~4.5 mm. Photo: R. Macphail and P. Goldberg.

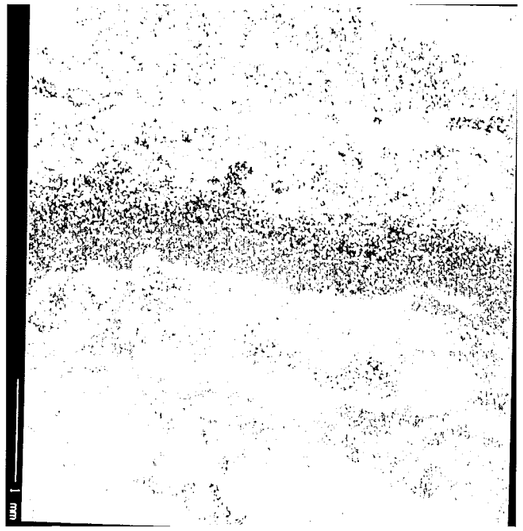

Fig. 13.26 As Fig. 13.25, microprobe elemental map: Van 97/52, layer 6a; Ca in guano – micro-facies *Gii*. Frame width is ~4.5 mm. Photo: R. Macphail and P. Goldberg.

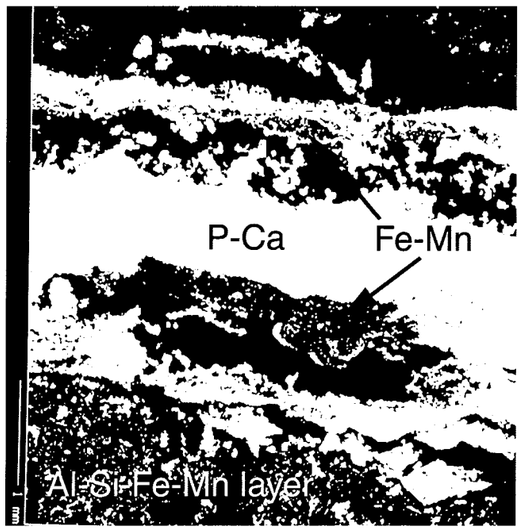

Fig. 13.27 As Fig. 13.26, microprobe elemental map: Van 97/52, layer 6a; Ca-P (35.35%) in guano – micro-facies *Gii*, with layers of mixed Al-Si-Fe-Mn and Fe-Mn. Frame width is ~4.5 mm. Photo: R. Macphail and P. Goldberg.

Fig. 13.28 Microprobe elemental map: Van 97/52, layer 6c; Mn-P-Ca in guano – micro-facies *Gi*. Phosphorus is mapped as P (0.96%), P-Ca (25.91%), P-Mn (0.15%) and P-Mn-Ca (6.20%). Frame width is ~8 mm. Photo: R. Macphail and P. Goldberg.

from these putative dunes. Massive sands are typically interbedded with silts, which may overall represent cyclical/seasonal climatic/weather (i.e. wetter/drier) fluctuations.

***Si* Silts**: These are finely bedded, and may contain planar voids that are presumably pseudomorphs of plant remains. The proposed origin of the silts (e.g. Van 97-53), as derived from surface soils washed through fissures in the karstic system, is supported by their relatively low LOI values (even compared to the sands), and apparently high magnetic susceptibility values. As burned sediments are not obviously present outside the areas of combustion features, they therefore are the likely result of in-wash of long-weathered and strongly oxidized Red Mediterranean (*terra rossa*) soils (Collins *et al.* 1994; Crowther, University of Wales Lampeter, pers. comm.). The occasional fine bone and charcoal content ultimately

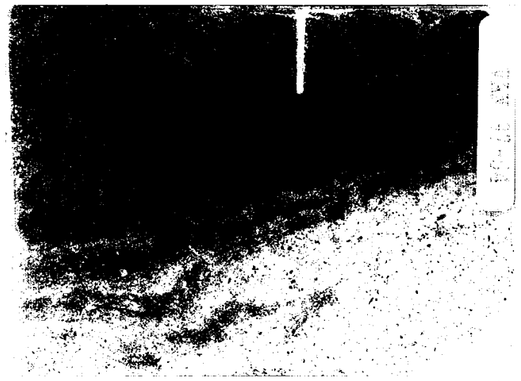

Fig. 13.29 Micromorphology sample Van 97/54 thin-section scan. Middle Area (context 156), showing some of the charcoal-rich lenses of the combustion zone (facies *CZ*); sample layers a–d were collected in the field (see text, Tables 13.2 and 13.5), over rubefied sands (facies *S*). This complex hearth feature, with very locally transported sedimentary hearth deposits, infills a depression (note layering), which then became a new *in situ* hearth. The magnetic susceptibility profile is as follows: χ = 234, 223, 128 and 90 x 10-8 Si/Kg, and demonstrates very clearly a reuse of the combustion zone/hearth. Width is ~75 mm. Photo: R. Macphail and P. Goldberg.

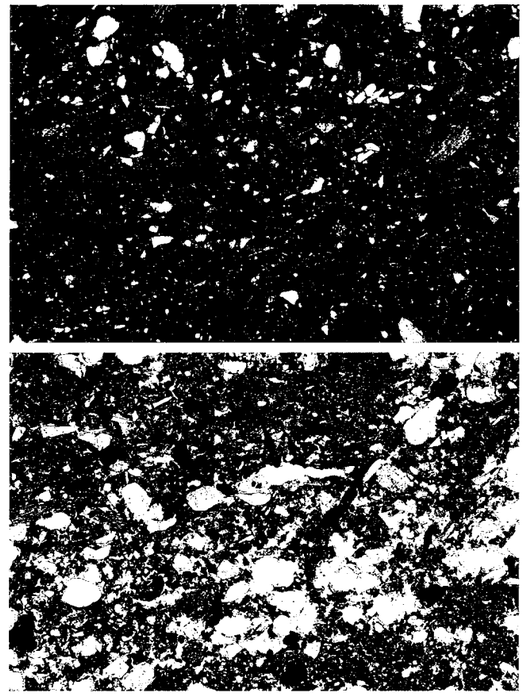

Fig. 13.30a and b Photomicrograph(s) of layered hearth deposits from Van 97/54, showing local redistribution of combustion zone (micro-facies CZ) organic silts and clays.
Top: Upper layer of dark brown bedded charred (blackened and rubefied) organic silt and clay, showing increasing amounts of blown sand upwards. XPL, frame width is ~3 mm.
Bottom: Lower layer of beige-coloured (and less burned) bedded organic silts and clays, with few intercalated blown sand. PPL, frame width is ~3 mm. Photo: R. Macphail and P. Goldberg.

represents the influence of fauna and humans within the cave (see hearths and combustion zones).

***G* Guano**: The chief guano layer at Vanguard Cave is present towards the top of the sequence in the Upper Area B (Fig. 13.2), which was studied in detail in long monolith sample 52 (Table 13.1; Fig. 13.4). This sample is generally organic and extremely phosphate rich because of its guano content. This material is autofluorescent under blue light implying an inorganic hydroxyapatite mineralogy as can be shown for guano deposits investigated in other caves (Karkanas *et al.* 2000; Wattez *et al.* 1990). Two main micro-facies are recognized. The first comprises dark stained biologically worked/burrowed guano layers (Gi) showing mixing of calcium phosphate-rich guano and other mineral material of anaerobic origin that is dominated by iron and manganese (Figs. 13.21–13.24). In contrast, massive, homogeneous grey- coloured guano layers (Gii) are very pure, layered calcium phosphate representing undisturbed surface accumulation of guano intercalated with cave earth and blown sand deposition and now Fe-Mn-replaced probable organic matter layers (Figs. 13.25–13.27). The presumed source of guano is from birds and these are not uncommon elements in the cave fauna (Chapter 17). Numerous recent studies have been made of cave phosphates in contexts that stretch from temperate Europe (Macphail and Goldberg 1999; Andrews 1990) down to the Mediterranean (Goldberg and Macphail 2006; Courty *et al.* 1989). In the latter region, bone, ashes and other sediments in Pleistocene caves have been replaced by a variety of secondary phosphates (Weiner *et al.* 1995), and it is possible that at Vanguard Cave some examples of Gii result from the similar replacement of ash. Inputs of guano are also recorded in some combustion zones (samples V96-19a/19c and V97-54a), contributing to phosphate levels.

***H* Hearths and Combustion zones**: Combustion zones and hearths occur as barely disturbed ash layers overlying rubified sediments. One good example is the hearth at the base of the shell midden in Area B (sample Van 97-51; Table 13.6; Figs. 13.10, 13.11 and 13.31); another is from the Middle Area (context 156). Both of these show layered, rubified and charcoal-rich 'silts' (sample Van 97-54; Table 13.6; Figs. 13.29 and 13.30). There are also examples of guano and phosphate transformed deposits (Figs. 13.21 and 13.22). These findings show that human occupation and burning activity took place on both sandy and silty substrates. It is also worth noting that the 50 mm thick succession of burnt silts and sands making up Van 97-54 (the combustion feature in context 156) demonstrates likely repeated episodes of use. This inference is further indicated by the magnetic susceptibility values of the washed CZ deposits which increase upwards, implying final heating of this multi-laminated combustion zone deposit (Table 13.6; Fig. 13.33a and b).

The presence of charcoal in sample Van 97-52 and traces of possible ash also indicates that the reddish brown guano deposits (Gi; Figs. 13.22–13.24) are most likely the result of

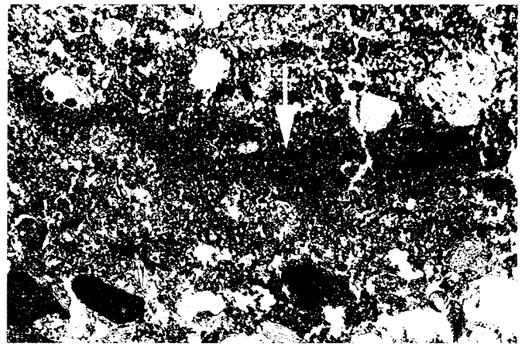

Fig. 13.31 Photomicrograph of Van 97/5I (see Fig. 13.11); mainly coarse calcite wood ash crystals including a thin layer of welded ash, forming a thin pan-like feature (arrow). This well-preserved *in situ* CZ micro-facies can be compared to the CZ formed in silts. PPL, frame width is ~3 mm. Photo: R. Macphail and P. Goldberg.

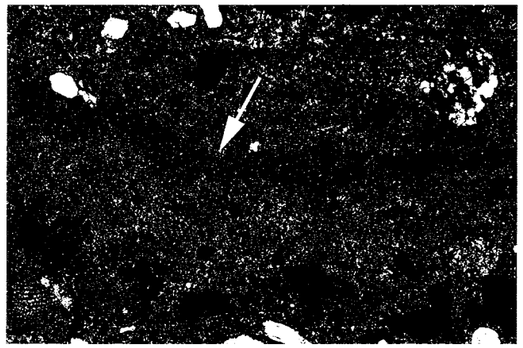

Fig. 13.32 As Fig. 13.3I, in XPL; slightly lower birefringence of the welded ash layer (arrow), probably indicates minor weathering of the hearth; note the few blown sand grains present. Here the hearth is located on, and buried by, sand. Photo: R. Macphail and P. Goldberg.

rubefaction by heating. On the other hand, the Gii layer mentioned above (Figs. 13.25–13.28) could constitute the phosphatized remains of an earlier ash layer (cf. Schiegl *et al.* 1996). Both of these observations are interesting because they indicate a human presence despite the absence of any lithic artefacts or other archaeological evidence. In combustion feature 150 it can be noted that the ashy brown unit (150b) is the most phosphorus-rich (4860 ppm P, Table 13.6, sample Van 96-19b).

Microprobe analysis at Vanguard Cave showed that sediments can be influenced by the mobilization, leaching and redeposition of iron and manganese (cf. Hill and Forti 1997).

Our present thinking substantiates the thoughts of Waechter (1951) by postulating a coastal environment dominated by a large dune system. At Vanguard Cave, for instance, the entire accumulation of ±17 m of sediments is overall inclined toward the rear of the cave, suggesting that the bulk of the sand mass would have been situated further seaward when sea-levels were lower. Furthermore, the sand is interspersed with silty washed accumulations, which gave rise to the interbedding of the sands and silts. Aeolian and sheet wash processes moved and reworked many of the sediments associated with Middle Palaeolithic occupation layers, resulting in slight redistribution of artefacts and hearth material. Within Vanguard Cave, only three, unequivocal *in situ* areas tied to use of fire were recognized. Although it is clear that there was probably a constant rain of guano and phosphate, much of this was diluted by dune sand accumulation. On the other hand, the preservation of ephemeral surfaces with evidence of combustion can show that some of these display guano concentrations, and it is possible that as in sample Van 97-52 a combustion zone was transformed by phosphatization associated with later guano inputs. In one of the hearths (the midden deposit, sample Van 97-51) scavenging by canids is recorded by the presence of coprolites (sample 371; Chapter 19). This type of scavenging and associated disturbance of occupation surfaces is well known from a number of other soil micromorphological studies of hunter and gatherer sites (Goldberg and Byrd 2000; Goldberg *et al.* 2007). The well preserved nature of hearths and reused hearth features argues strongly in favour of very rapid sedimentation rates.

Conclusions

This detailed study, supported by analysis of soil micromorphology and chemistry, has brought to light a number of depositional and post-depositional processes linked to geogenic, biogenic and anthropogenic activities. The major findings can be summarized within two broad categories:

Cave sedimentation

Sediments at Vanguard Cave are less phosphatic and organic, and generally have undergone fewer diagenetic changes

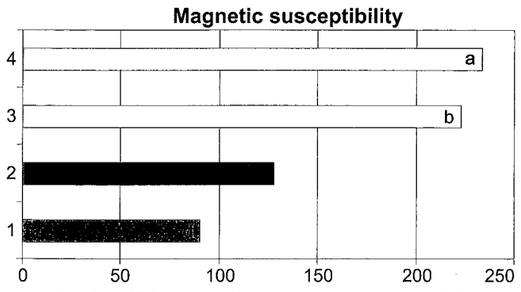

Fig. 13.33a Van 97/54 sample layers a–d; magnetic susceptibility sequence, demonstrating probable *in situ* burning of these layers.

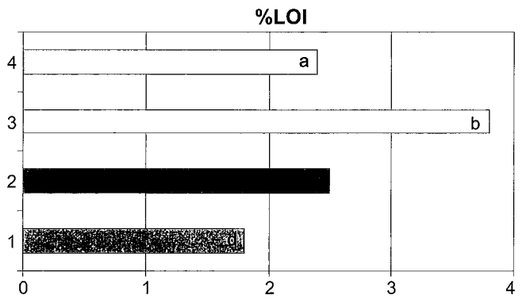

Fig. 13.33b Van 97/54 sample layers a–d; percentage LOI sequence.

compared to Gorham's Cave (Chapters 2–4). Exceptionally well preserved *in situ* hearth deposits with ash layers survive in Vanguard Cave, with one example showing rapid burial by blown sand. Although sedimentation is affected by probable seasonal/climatic fluctuations in cave water, it is interesting that karstic activity, for example the formation of speleothems, is absent (at least near the present front) in Vanguard Cave, despite the evident occurrence of water-lain silts. Animals, especially birds, have contributed far less substantially to organic and phosphatic sedimentation, in comparison to Gorham's Cave. Their deposits (organic matter, guano, phosphate) have been generally strongly diluted by rapid dune sand deposition, but concentrations are evident where ephemeral surfaces and associated hearths and combustion zones occur on silts for example. These impermanent surfaces were subjected to intense biological activity, including the presence of humans, and also affected by local (very shallow) erosion and colluviation. However, the degree and vertical range of bioturbation is relatively low in all observed sections. Indeed, in the Middle Area (adjacent to hearth 150), the fine stratigraphic detail continues right to the cave wall.

Human activity

From the microstratigraphic analysis of the hearths, there is compelling evidence that Neanderthals reused these features. We have also noted that they apparently showed no preference for occupying sandy or silty substrates.

Acknowledgements

The authors thank the National Geographic Society for funding this research, and the Natural History Museum and Gibraltar Museum for discussion, collaboration and support especially through Chris Stringer and Clive Finlayson, respectively. The Institute of Archaeology, University College London is also thanked for support especially through Sandra Bond (SEM/EDXRA), Kevin Reeves (microprobe) and Cyril Bloomfield (analysis of Phosphorus); additional analyses including magnetic susceptibility were carried out by Johan Linderholm (Environmental Archaeology Laboratory, Umeå University, Sweden), who is gratefully acknowledged. Thin sections were manufactured by Spectrum Petrographics (Vancouver, Washington, USA). In addition we gratefully thank the following for their contribution to this study: Peter Andrews, Gerry Black, Andy Currant, Clive and Geraldine Finlayson, Lorraine Cormish, Jo Cooper, Yolanda Fernández-Jalvo, Frank Greenway and Chris Stringer.

References

Andrews, P. 1990: *Owls, Caves and Fossils* (London, Nat. Hist. Mus. Publications).

Barton, R. N. E. 2000: Mousterian Hearths and Shellfish: Late Neanderthal Activities on Gibraltar. In Stringer, C. B., Barton, R. N. E. and Finlayson, J. C. (eds.), *Neanderthals on the Edge* (Oxford, Oxbow Books), 211–220.

Bullock, P., Fedoroff, N., Jongerius, A., Stoops, G., Tursina, T. and Babel, U. 1985: *Handbook for Soil Thin Section Description* (Wolverhampton, Waine Research).

Collins, M. B., Gose, W. A. and Shaw, S. 1994: Preliminary geomorphological findings at Dust and nearby caves. *Journal of Alabama Archaeology* 40, 35–56.

Courty, M. A., Goldberg, P. and Macphail, R. I. 1989: *Soils and Micromorphology in Archaeology* (Cambridge, Cambridge University Press).

Davies, W., Stewart, J. and van Andel, T. H. 2000: Neanderthal landscapes – a preview. In Stringer, C. B., Barton, R. N. E. and Finlayson, J. C. (eds.), *Neanderthals on the edge* (Oxford, Oxbow Books), 1–8.

Fernández-Jalvo, Y. and Andrews, P. 2000: The taphonomy of Pleistocene caves, with particular reference to Gibraltar. In Stringer, C. B., Barton, R. N. E. and Finlayson, J. C. (eds.), *Neanderthals on the Edge* (Oxford, Oxbow Books), 171–182.

Finlayson, C. and Pacheco, F. G. 2000: The southern Iberian peninsula in the late Pleistocene: geography, ecology and human occupation. In Stringer, C. B., Barton, R. N. E. and Finlayson, J. C. (eds.), *Neanderthals on the Edge* (Oxford, Oxbow Books), 139–154.

Goldberg, P. and Byrd, B. 2000: The interpretive potential of micromorphological analysis at prehistoric shell midden sites on Camp Pendleton. *Pacific Coast Archaeological Society Quarterly* 35(4), 1–23.

Goldberg, P. and Macphail, R. I. 2000: Micromorphology of sediments from Gibraltar caves: some preliminary results from Gorham's Cave and Vanguard Cave. In Finlayson, C., Finlayson, G. and Fa, D., *Gibraltar during the Quaternary* (Gibraltar, Gibraltar Government Heritage Publications, Monograph 1), 93–108.

Goldberg, P. and Macphail, R. I. 2006: *Practical and Theoretical Geoarchaeology* (Oxford, Blackwell Publishing).

Goldberg, P., Macphail, R. I. and Homburg, J. 2007: *Playa Vista Archaeological and Historical Project (California): soil micromorphology report* (Tucson, Statistical Research Inc.).

Hill, C. and Forti, P. 1997: *Cave Minerals of the World* (Huntsville, National Speleological Society).

Holiday, V. T. 2004: *Soils in Archaeological Research* (Oxford, Oxford University Press).

Karkanas, P., Kyparissi-Apostolika, N., Bar-Yosef, O. and Weiner, S. 2000: Mineral assemblages in Theopetra, Greece: a framework for understanding diagenesis in a prehistoric cave. *Journal of Archaeological Science* 26, 1171–1180.

Linderholm, J. 2007: Soil chemical surveying: a path to a deeper understanding of prehistoric sites and societies in Sweden. *Geoarchaeology* 22, 417–438.

Macphail, R. I. and Goldberg, P. 1999: The soil micromorphological investigations of Westbury Cave. In Andrews, P., Cook, J., Currant, C. and Stringer, C. (eds.), *Westbury Cave. The Natural History Museum Excavations 1976–1984* (Bristol, CHERUB), 59–86.

Macphail, R. I. and Goldberg, P. 2000: Geoarchaeological investigation of sediments from Gorham's and Vanguard Caves, Gibraltar: microstratigraphical (soil micromorphological and chemical) signatures. In Stringer, C. B., Barton, R. N. E. and Finlayson, J. C. (eds.), *Neanderthals on the Edge* (Oxford, Oxbow Books), 183–200.

Meignen, L., Bar-Yosef, O. and Goldberg, P. 1989: Les

Structures de Combustion Moustériennes de la Grotte de Kébara (Mont Carmel, Israel). *Mémoires Du Musée de Préhistoire d'Ile de France* 2, 141–146.

Murphy, C. P. 1986: *Thin Section Preparation of Soils and Sediments* (Berkhamsted, A B Academic Publishers).

Schiegel, S. G., Goldberg, P., Bar-Yosef, O. and Weiner, S. 1996: Ash mineralogical observations and their archaeological implications. *Journal of Archaeological Science* 23, 763–781.

Stoops, G. 1996: Complementary techniques for the study of thin sections of archaeological materials. In Castelletti, L. and Cremaschi, M. (eds.), *XIII International Congress of Prehistoric and Protohistoric Sciences Forlì-Italia-8/14 September 1996, 3 Paleoecology* (Forlì, A.B.A.C.O.), 175–182.

Stoops, G. 2003: *Guidelines for Analysis and Description of Soil and Regolith Thin Sections* (Madison, Wisconsin, Soil Science Society of America, Inc.).

Stringer, C. B., Finlayson, J. C., Barton, R. N. E., Fernández-Jalvo, Y., Caceres, I., Sabin, R., Rhodes, E. J., Currant, A. P., Rodriguez-Vidal, J., Giles Pacheco, F. and Riquelme Canatal, J. A. 2008: Early Neanderthal exploitation of marine mammals, Quaternary Science Reviews. *Proceedings of the National Academy of Sciences USA* 105(38), 14319–14324.

Waechter, J. d'A. 1951: The excavation of Gorham's Cave, Gibraltar: preliminary report for the seasons 1948 and 1950. *Proceedings of the Prehistoric Society* NS 17, 83–92.

Wattez, J., Courty, M. A. and Macphail, R. I. 1990: Burnt organomineral deposits related to animal and human activities in prehistoric caves. In Douglas, L. A. (ed.), *Soil Micromorphology: a basic and applied science* (Amsterdam, Elsevier), 431–441.

Weiner, S., Goldberg, P. and Bar-Yosef, O. 1993: Bone Preservation in Kebara Cave, Israel Using On-Site Fourier Transform Infrared Spectrometry. *Journal of Archaeological Science* 20, 613–627.

Weiner, S., Schiegel, S. G., Goldberg, P. and Bar-Yosef, O. 1995: Mineral assemblages in Kebara and Hayonim Caves, Israel: Excavation strategies, bone preservation and wood ash remnants. *Israel Journal of Chemistry* 35, 143–154.

14 OSL age estimates from Vanguard Cave

E.J. Rhodes

Introduction

Two suites of sediment samples were collected for OSL dating from which a total of seven were measured in this study. One sample, laboratory code X369, field code VAN98-OSL8, was part of a suite collected in 1998 using steel tubes; OSL results reported by Pettitt and Bailey (2000) also formed part of the same sample suite. A second suite was collected in August 2001, by pushing opaque black PVC tubes into cleaned sediment sections. During the 2001 visit, *in situ* NaI gamma fspectrometer measurements were made at each sampling location (including several 1998 locations), in order to provide a direct measurement of gamma dose rate. Standard sample preparation methods (described in detail below) were used to extract quartz grains from each sediment, and these were measured using a conventional multiple grain single aliquot regenerative-dose (SAR) protocol (Murray and Wintle 2000, 2003).

For several samples, the sediment was observed to be well sorted, clean medium to coarse sand, some having a prominent shell fragment component, while other samples were collected in finely laminated interbedded silts and fine to medium sands. The deposits appear to contrast with the lower part of the Gorham's Cave sequence however. This may be explained partly by the generally much higher sedimentation rate and lower bioturbation level in Vanguard Cave than in Gorham's (Collcutt, pers. comm.). In parallel with these observations, the measured OSL single aliquot equivalent dose distributions from the Vanguard Cave samples were generally much more tightly grouped than those from Gorham's Cave, giving the impression of less incomplete bleaching at deposition, and less post-depositional mixing of grains from different horizons and of different ages. These combined observations lead the author to have a greater degree of confidence in these multiple grain SAR determinations from Vanguard Cave than those measured in Gorham's Cave (Chapter 6), which were demonstrated by subsequent single grain measurements to suffer from incomplete zeroing and post-depositional mixing.

In order to confirm this interpretation, and to confirm the veracity of the OSL age model, single grains were measured for sample X729 (field code VAN01-U01), collected at the same location as Pettitt and Bailey's VAN 1 (see below), relatively high in the stratigraphy and a key location for assessing the apparent age disagreement with both the radiocarbon and OSL determinations of Pettitt and Bailey (2000). The measured single grain age distribution confirms only a degree of incomplete zeroing for this sample, and lends support to an older chronology for sediment deposition in comparison to that published (Pettitt and Bailey 2000). The stratigraphic position of this key sample places a minimum age constraint on the sediments beneath, which represent the majority of the deposits preserved within the cave, and the age estimate suggests that most of the sequence was deposited within or before MIS 5.

The seven samples measured span the main bulk of sediments within the cave, and provide an age model for some of the more important archaeological horizons, including layers associated with the working of marine mammals (Stringer *et al.* 2008). The present paper represents a formal record of the procedures used and the results obtained. At this stage, it is not necessarily considered a definitive statement of the age of these sediments, and important points are made in the discussion, below. As there was a degree of incomplete zeroing witnessed by single grain measurements for sample X729, it seems likely that other samples in this sequence may suffer from similar, relatively modest, age overestimation caused by this effect.

Sample location, preparation and measurement

Sample locations are shown by context number in Table 14.1, and graphically in Figure 14.1. Samples were opened in controlled laboratory lighting within the Research Laboratory for Archaeology and the History of Art (RLAHA), Oxford, UK and the outer 1 to 2 cm from both ends used for water content determination and NAA measurement. The inner sediment from each tube was treated with dilute HCl to remove carbonate and disaggregate grains. Samples were wet sieved, and grains of between 180 and 255 μm were treated in concentrated (40%) HF plus HCl, continuously agitated for around 100 minutes. This treatment removes feldspar grains and etches the surface of each quartz grain. After rinsing and drying, each sample had heavy minerals removed using a sodium polytungstate solution, density 2.68 $g.cm^{-3}$. The remaining quartz-rich lighter fraction was rinsed and dried, and sieved a second time to remove grains smaller than 180 μm. For conventional multiple grain measurement, grains were mounted on 9.7 mm diameter aluminium or stainless steel discs using a viscous silicone oil, with the sample covering approximately the central 5 mm, corresponding to around 300 grains per aliquot. For single grain OSL measurement, sample X729 was re-sieved using a 212 μm mesh, and only the finer fraction used.

Preheating was conducted at 260°C for 10s before natural and regenerative-dose OSL measurements and a heat treatment of 220°C for 10s before each sensitivity measurement was used. Routine assessment of IRSL as a measure of feldspar contamination demonstrated only negligible signals (<0.5% OSL). All measurements were made